PCCP

Accepted Manuscript

ROYAL SOCIETY OF CHEMISTRY

www.rsc.org/pccp

Theoretical Study of the Reactions of Criegee Intermediates with Ozone, Alkylhydroperoxides, and Carbon Monoxide

L. Vereecken,[a*] A. R. Rickard,[b,c] M. J. Newland,[d,e] W. J. Bloss[d]

[a] Max Planck Institute for Chemistry, Hahn-Meitner-Weg 1, Mainz, Germany

[b] National Centre for Atmospheric Science (NCAS), University of York, York, UK

[c] Wolfson Atmospheric Chemistry Laboratories, Department of Chemistry, University of York, York, UK

[d] School of Geography, Earth and Environmental Sciences, University of Birmingham, Birmingham, UK

[e] University of East Anglia, School of Environmental Sciences, Norwich, UK

* Corresponding author email: Luc.Vereecken@mpic.de

Abstract

The reaction of Criegee intermediates (CI) with ozone, O_3, has been re-examined with higher levels of theory, following earlier reports that O_3 could be a relevant sink of CI. The updated rate coefficients indicate that the reaction is somewhat slower than originally anticipated, and is not expected to play a role in the troposphere. In experimental (laboratory) conditions, the CI + O_3 reaction can be important. The reaction of CI with ROOH intermediates is found to proceed through a pre-reactive complex, and the insertion process allows for the formation of oligomers in agreement with recent experimental observations. The CI + ROOH reaction also allows for the formation of ether oxides, which don't react with H_2O but can oxidize SO_2. Under tropospheric conditions, the ether oxides are expected to re-dissociate to the CI + ROOH complex, and ultimately follow the insertion reaction forming a longer-chain hydroperoxide. The CI +ROOH reaction is not expected to play a significant role in the atmosphere. The reaction of CI with CO molecules was studied at very high levels of theory, but no energetically viable route was found, leading to very low rate coefficients. These results are compared

against an extensive literature overview of experimental data.

Table of Content Graphic

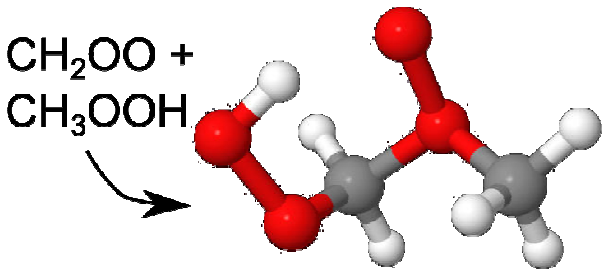

The reaction of Criegee intermediates with hydroperoxides yields exotic ether oxides, as well as oligomers.

1. Introduction

Carbonyl oxides, also known as Criegee intermediates (CI), are strong oxidants formed in the ozonolysis of alkenes. Their role in the ozonolysis reaction is well-understood,[1–3] where they act as key intermediates allowing access to the formation of OH radicals through the vinylhydroperoxide channel, or the formation of esters and acids through the ester channel. Their fate depends strongly on their nascent energy content, i.e. chemically activated CI undergo fast unimolecular reactions as described above, while CI with a thermal energy content, called stabilized Criegee intermediates (SCI), have a sufficiently long lifetime to also undergo bimolecular reactions. The yield of SCI from ozonolysis reactions is still subject to large uncertainties, and depends on pressure and temperature. Furthermore, ozonolysis of substituted alkenes can give rise to different conformers of SCI, e.g. *syn*-CH_3CHOO and *anti*-CH_3CHOO from 2-butene + O_3; the relative yield of these species in ozonolysis reactions remains often speculative. The incorporation of SCI chemistry into chemical kinetic models is further complicated by the observation that SCI with different substituents, and even different conformers of SCI with identical substituents, can show highly distinct chemistry, with rate coefficients for individual reactions differing by several orders of magnitude.[2,4–10] In recent years, since the first direct detection of H_2COO by Taatjes et al. in 2008,[11] many experimental determinations have become available,[6,12–29] including the rates of the reactions with H_2O, $(H_2O)_2$, SO_2, NO_2, NO, aldehydes, carboxylic acids, alkenes, and others. Theoretical work[2,5,30–39] spans an even larger set of co-reactants including RO_2 and HO_2 radicals, and ozone; theory thus remains an invaluable source of information on the relative rates for Criegee intermediates or co-reactants that are not readily accessible in the lab, as well as characterizing the temperature- and pressure-dependence for some of the reactions. Still, even with the available data, it remains difficult to assess the impact of SCI chemistry in the free troposphere, or in

indoor environments. Large uncertainties remain on rate coefficients and product distributions, and even on which co-reactants are critical in determining the (steady-state) concentration of the SCI. This is particularly well illustrated by the multiple estimates of the fate of CI in the atmosphere by Novelli et al.,[5,21,30] where the availability of new data over the last years has regularly changed the estimated relative contribution of the respective co-reactants.

In this work, we study a number of reactions thought to be of importance in the atmosphere or in laboratory investigations. The reaction of SCI with ozone was proposed in earlier work,[5,33,35] where theoretical work by Kjaergaard et al.[33] derived a lower limit for $H_2COO + O_3$ of 10^{-18} cm^3 $molecule^{-1}$ s^{-1} for the rate coefficient at room temperature. Wei et al.[35] claim this reaction occurs easily in the atmosphere, yet their predicted reaction barrier of 14.1 kcal mol^{-1} implies rate coefficients of less than ~10^{-20} cm^3 $molecule^{-1}$ s^{-1} at 298 K. In contrast, Vereecken et al.[5] derived a rate coefficient as high as 10^{-12} cm^3 $molecule^{-1}$ s^{-1}. This latter rate coefficient would imply that this reaction can be of importance in the atmosphere, and would have played an unquantified role in many ozonolysis experiments. In this work, we apply higher levels of theory to this reaction, as well as extending our study to more complex SCI. Alkylhydroperoxides, ROOH, and hydrogen peroxide, HOOH, are both present in the atmosphere in measurable quantities,[40–42] especially in more pristine regions where a significant fraction of peroxy radicals, RO_2 –formed in the oxidation of volatile organic compounds, VOC– react with hydroperoxy radicals, HO_2, as opposed to with NO as in polluted areas. Reaction of SCI with ROOH has been proposed recently as a source of peroxide oligomers observed in ethylene ozonolysis,[43] offering an alternative peroxide oligomer formation route to the earlier proposed CI + RO_2 reaction.[44,45,30,31]

Carbon monoxide, CO, is a ubiquitous molecule both in the atmosphere and under many experimental conditions. Recent theoretical work by Kumar et al.[34] found that the reaction barriers for its reaction with SCI are high, with a very low predicted rate coefficient, k(298K) = 6.4×10^{-23} cm^3

molecule^{-1} s^{-1}. Our own earlier independent theoretical work[46] found several additional reaction channels not included in the work by Kumar et al. Furthermore, CO has been used as an SCI scavenger in experiments,[47] implying a reasonably high rate coefficient, which appears to be in disagreement with the theoretical predictions. In this work, we therefore present a significantly extended examination of the SCI + CO reaction, including an extensive overview of experimental data available for this reaction.

Prior to discussing our results, we summarize some properties of oxides of oxygen-bearing molecules, more specifically carbonyls, water, alcohols and ethers, as these oxides and their specific properties are important in the chemistry discussed in this work. SCI, carbonyl oxides, have a 1,3-dipole structure that has a predominantly zwitterionic structure, with 4 electrons in the π-system:

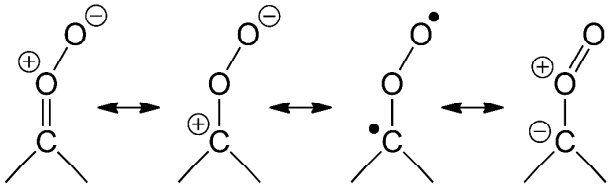

The partial double bond character of the central C–O bond prohibits fast rotation of the outer oxygen, with a barrier above 25 kcal mol^{-1},[2] such that the conformers with *syn*- and *anti*- orientations effectively act as separate chemical species at atmospheric temperatures. SCI are selectively reactive, i.e. they will react very fast with carboxylic acids, carbonyl compounds, SO_2, NO_2, etc., but their reactions with e.g. H_2O, NO, or VOCs is slow.

H_2OO, water oxide (or oxy-water), is a 1,2-dipole that has been observed experimentally.[48] This ylide is known to be unstable towards 1,2-H-migration back towards its tautomer hydrogen peroxide,[49–51] HOOH, with a barrier of only ~ 3-4 kcal mol^{-1}. Upon replacing H-atoms in oxywater with alkyl groups, one obtains alcohol oxides, RO(O)H and ether oxides, RO(O)R', which are less well understood than water oxide.

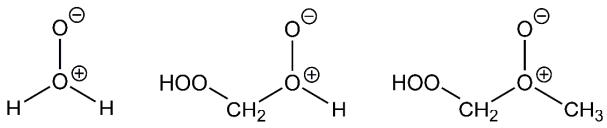

Water oxide | Alcohol oxide (from CI + HOOH) | Ether oxide (from CI + CH_3OOH)

We are aware of only one theoretical study on ether oxides, by Schalley et al.,[52] who found that alcohol oxides are also likely to undergo a 1,2-H-migration, forming the hydroperoxide after clearing a barrier of ~ 5 kcal mol^{-1}. Ether oxides were found to be significantly more stable towards isomerisation, with barriers exceeding 25 kcal mol^{-1}. Similar to CI and O_3, these ylides are expected to be powerful oxidizing agents.

2. Methodology

2.1. Quantum chemical calculations

The geometries for all structures were optimized using the M06-2X/aug-cc-pVTZ methodology,[53,54] while for a subset of the calculations we also performed geometry optimizations using CCSD and CCSD(T)[55,56] calculations based on the (aug-)cc-pVDZ and/or (aug-)cc-pVTZ basis sets.[54] The relative energies were further improved using single point calculations on these geometries, using ROHF-CCSD(T) calculations with Dunning aug-cc-pVxZ (x=D, T and/or Q) basis sets,[30] where extrapolation to infinite basis sets was done for some of these structures based on the Schwartz schemes proposed by Martin et al.,[57] specifically the two-point aug-Schwartz4 and the three-point aug-Schwartz6 extrapolation based on CCSD(T)/aug-cc-pVxZ (x=D,T,Q) data. Harmonic vibrational wavenumbers were obtained by M06-2X/aug-cc-pVTZ on geometries at that same level of theory in all cases, using a scaling factor of 0.971 for the zero-point vibrational energy.[58,59] All DFT calculations used a pruned ultrafine integration grid with 99 radial and 590 angular points, and very tight SCF convergence

criteria. Many structures were also examined using broken-symmetry[60,61] M06-2X calculations to search for singlet biradical structures and pathways. Finally, IRCMax[62] calculations were performed to examine the skew between the PES at DFT and CCSD(T) level of theory.

Only single-reference methodologies are used here, even though many of the intermediates are intrinsically multi-reference; still, the methods used here are usually found to perform adequately.[2,63] For carbonyl oxides, broken-symmetry unrestricted SCF wave functions converged to the dominant zwitterionic closed shell wavefunction, yielding the same results as for restricted-spin singlet calculations. For ozone, open-shell singlet M06-2X calculations yield a spin density separation across the outer oxygen atoms, which implies a stronger contribution of the bi-radical component in the wavefunction; S^2 remains ≤0.01 after annihilation of the first spin contaminant. T1 diagnostics, a measure of the multi-reference character of the wavefunction, are listed in the supporting information; structures with values above 0.044 are expected[64] to benefit from multi-reference methodologies. For the structures studied here, the T1 diagnostics remained below this value, except for the Criegee intermediates where it reaches values as high as 0.0477. The restrictions on wavefunction flexibility when applying single-reference methodologies to these compounds will lead to an overestimation of the energy, i.e. better levels of theory would allow the reactants in the title reactions to have a lower relative energy compared to the products. The good agreement of many theoretical predictions with experimental data on CI reactions suggests this effect is minor for the CI studied here.[2,63]

All quantum chemical calculations were performed using Gaussian-09.[65]

2.2. Theoretical kinetic analysis

Rate coefficients for all reactions are calculated using canonical TST, in a rigid rotor harmonic

oscillator approximation :

$$k(T) = \frac{k_B T}{h} \frac{Q^{TS}(T)}{Q^{react}(T)} \exp\left(\frac{-E_b}{k_B T}\right)$$

While several of the reactions show a pre-reactive complex, and even slightly submerged addition TS, the reactions proceed significantly slower than the formation and redissociation of the pre-reactive complex, establishing a steady-state population for the complex and effectively canceling the complex out of the rate equation. Tunneling corrections were not performed, as all reactions have a high reduced mass along the reaction coordinate, preventing efficient tunneling ; many of the reaction TS additionally show a low, broad energy profile that is unpropitious for tunneling.

3. CI + O_3

3.a. The potential energy surface

Figure 1 shows the potential energy of the O_3 + H_2COO reaction, adapted from Vereecken et al.[5] In this work, we focus on the initial addition transition states of the CI + O_3 reaction for various (substituted) CI. Analogous to the CI + H_2COO reaction, we propose that for all these reactions the products are ultimately a carbonyl compound with 2 O_2 molecules. Table 1 lists the pre-reactive complex stabilities, barrier heights and rate coefficients for the reactions examined here, at the highest available level of theory.

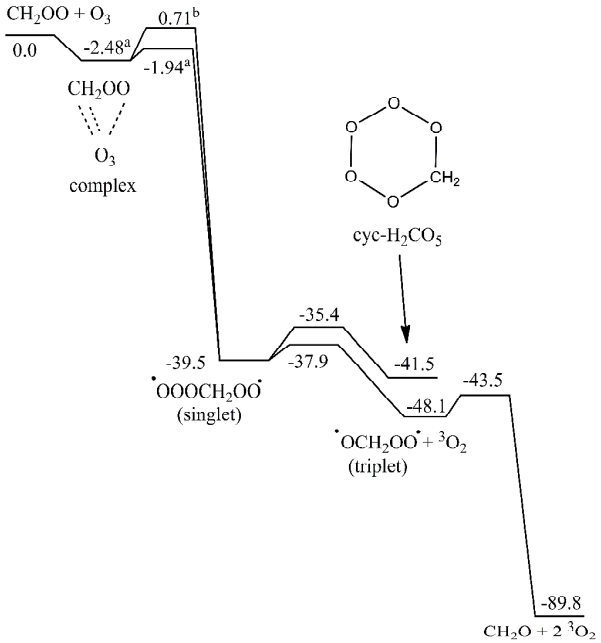

Figure 1: Potential energy surface (kcal mol^{-1}) of the CH_2OO + ozone reaction at the ROCCSD(T)/aug-cc-pVTZ//M06-2X/aug-cc-pVTZ level of theory. The entrance TS are at higher levels of theory : (a) ROCCSD(T)/aug-Schwartz6(DTQ)//M06-2X ; (b) obtained relative to (a) using ROCCSD(T)/aug-Schwartz4(DT) energies

Table 1: Relative energies (kcal mol^{-1}) of the pre-reactive complex, and the two TS conformers for chain addition in the CI+ O_3 reaction. Rate coefficients k(T) (cm^3 molecule^{-1} s^{-1}),where the Arrhenius expression is valid for T=250-350K.

CI	Complex	TS	k(298 K)	k(T)
H_2COO	-2.48[a]	-1.94[a] / 0.71[b,c]	4×10^{-13}	8×10^{-14} exp(487/T)
syn-CH_3CHOO	-3.93[c]	-0.60[c] / 1.42[b,d]	3×10^{-14}	8×10^{-14} exp(-285/T)
anti-CH_3CHOO	-3.73[c]	-3.58[c] / 0.07[b,d]	3×10^{-12}	2.5×10^{-14} exp(1425/T)
$(CH_3)_2COO$	-5.15[d]	-1.51[c] / 1.18[b,d]	8×10^{-14}	3×10^{-14} exp(285/T)

[a] CCSD(T)/aug-Schwartz6(DTQ)//M06-2X/aug-cc-pVTZ ; [b] Based on energy relative to lowest TS ; [c] CCSD(T)/aug-Schwartz4(DT)//M06-2X/aug-cc-pVTZ ; [d] CCSD(T)/aug-cc-pVDZ//M06-2X/aug-cc-pVTZ

The pre-reactive complex was found to become more stable with increasing CI substitution, with $(CH_3)_2COO$ yielding a complex twice as stable compared to H_2COO. The trend for the transition states is less clear-cut, and appears to be affected by the interaction between the O_3 moiety and the methyl substituents. Increasing substitution leads to tighter TS, with the C–O distance for chain addition reducing from 2.44 Å for $H_2COO + O_3$ to 2.29 Å for $(CH_3)_2COO$. As already found for other reactions,[2,5] the large energy difference for the *syn*- and *anti*-CH_3CHOO barriers is mostly due to the energy difference between these conformers, where the absolute energy difference between the TS (~0.6 kcal mol^{-1}) is significantly less than that for the reactants (~3.5 kcal mol^{-1}), *i.e.* the higher potential energy in the high-energy *anti* conformer is mostly released in the TS. The difference between the rate coefficient for syn- and anti-CH_3CHOO is thus predicted to be as high as two orders of magnitude. The $^{\bullet}OOCH(CH_3)OOO^{\bullet}$ diradical adducts formed from these two CI are not distinguishable, as the peroxy radical moiety does undergo facile internal rotation. The barrier height predictions are found to be rather dependent on the level of theory used, with differences as high as 2.1 kcal mol^{-1} between single-point CCSD(T)/aug-cc-pVxZ calculations (x = D, T, and Q). This also implies that the extrapolations to complete basis set are less reliable, e.g. for CI + H_2COO, the aug-Schwartz4(DT) differs from the more reliable aug-Schwartz4(TQ) and aug-Schwartz6(DTQ) results by 0.5 kcal mol^{-1}, whereas the latter two only differ by 0.1 kcal mol^{-1}. It is likely that the underlying cause here is the use of the rather small aug-cc-pVDZ basis set, where larger basis sets allow for significant improvement in reliability of the calculations. To verify the impact of the TS geometry, we performed IRCMax calculations along the M06-2X reaction coordinate of $CH_2OO + O_3$, using CCSD(T)/aug-cc/pVxZ (x = D, T) single point energies. For the CC//aVDZ results, an energy maximum was found 1.32 Bohr $AMU^{0.5}$ beyond the TS, whereas for CC/aVTZ the maximum shifted to 1.58 Bohr $AMU^{0.5}$, with an energy 0.8 kcal mol^{-1} above the single point energy at the M06-2X TS geometry, yet still 2.1

kcal mol^{-1} below the free reactants. Again, the differences between the M06-2X, CC/aVDZ, CC/aVTZ and CC/aVQZ PES suggests that the barrier height predictions carry a significant uncertainty. From the above, we estimate the reliability of the barrier heights in Table 1 to be no better than 1.5 kcal mol^{-1} ; our highest levels of theory also yield the least-submerged barriers leading to the lowest rate coefficients. At the same time, the IRCMax calculations show unequivocally that a submerged pathway does exist at the CCSD(T) level of theory, connecting the pre-reactive complex to the adduct following the chain addition route. This confirms our earlier[5] conjecture that the CI + O_3 reaction proceeds via a chain addition process, as opposed to a cycloaddition as obtained by Kjaergaard et al.[33] and Wei et al.[35] based on B3LYP geometries, where the large barriers at the CCSD(T)//B3LYP level of theory,[35] exceeding 14 kcal mol^{-1}, clearly show that the cycloaddition pathway is energetically not the most optimal route. Furthermore, the cycloaddition process is entropically disfavored compared to the chain addition process. Finally, we attempted to re-optimize the addition TS at the CCSD(T) level of theory, but slow convergence, and the exceedingly high computational cost forced us to abandon this approach. We are currently likewise limited by computational power to perform more extensive CCSD(T) calculations than reported here.

It is interesting to note that the carbonyl species formed in this reaction, e.g. CH_2O from the CH_2OO + O_3 reaction, receives its oxygen atom from the ozone molecule, while the two SCI oxygen atoms are released as an O_2 molecule. Some oxygen atom scrambling occurs for the fraction of intermediates that pass through the cyclic isomer, but this channel is energetically and entropically disfavored. Isotopic labeling experiments could thus be used to confirm or disprove the chain addition mechanism proposed here, as the cycloaddition mechanism proposed by other authors[33,35] would lead to a ~1:1 ratio of carbonyl oxygen atoms originating from the SCI or O_3 moiety.

3.b. Reaction kinetics

The rate coefficients of the CI + O_3 reactions are listed in Table 1, all showing a negative or very small positive temperature dependence owing to the submerged TS of the rate-determining step. The Arrhenius expressions given should only be used in a narrow ±100K temperature interval around room temperature. At lower temperatures, the outer TS for complex formation becomes the rate determining step, invalidating the kinetic methodology used. The uncertainty on the barrier height (see above) is the main source of uncertainties; we estimate an uncertainty of at least 1 order of magnitude on the reaction rate. A key problem in the assessment of the error is the lack of higher-level benchmark calculations, which require a computational cost that is unattainable for us. Direct measurement of even a single CI + O_3 reaction would provide a much-needed point of reference. The recent experimental work by Novelli et al.[21] used our current *syn*-CH_3CHOO + O_3 rate coefficient in their kinetic model of alkene ozonolysis reaction systems with 480 ppb of O_3, finding a good agreement between predicted and measured OH generated from *syn*-CH_3CHOO decomposition. These experiments, however, were not particularly sensitive to the CI + O_3 rate coefficient, but rather to the total CI loss factoring into the establishment of a CI steady state concentration. Our CI-specific rate coefficient prediction combined with the literature value for CI loss did allow for good quantitative reproduction of the observations, whereas using a rate coefficient differing by an order of magnitude strongly diminished the agreement.

The predicted rate coefficients thus suggest that the CI + O_3 reaction can affect the reaction mixture in laboratory work. Novelli et al.[21] found earlier that the CI + O_3 reaction can be of minor importance in the troposphere, removing 1-2% of the CI. These results, however, were based for all SCI on the higher rate coefficient of 1×10^{-12} cm^3 $molecule^{-1}$ s^{-1} predicted at that time for CH_2OO + O_3. Using the current CI-specific predictions, we find that O_3 is negligible as a CI sink in the troposphere for the four SCI studied here, and that the CI steady-state concentration is determined by other loss processes such as the reaction with water, water dimer, acids, and unimolecular decomposition.

4. CI + ROOH

4.a. The potential energy surface

Figure 2 shows the PESs for the reactions of CH_2OO with H_2O_2 and CH_3OOH, and the reaction of $(CH_3)_2COO$ with CH_3OOH. In all cases, we found the formation of a fairly stable pre-reactive complex, at ~ 9 kcal mol^{-1} below the free reactants. For each complex, we find two accessible reaction channels. The first channel is an insertion reaction into the ROO–H hydroperoxide bond, leading to the formation of a longer ROOC(R')(R")OOH hydroperoxide. The insertion mechanism is similar to that found in the CI + H_2O and CI + ROH reactions,[2,7–9] and confirms the possibility of oligomer formation as observed by Sakamoto et al.[43] This channel shows a submerged barrier, and is likely to be accessible for all CI and ROOH combinations, as no specific steric hinderance effects are expected for joining the –OOH and >COO moieties, and H-bonding between the reactants readily allows for the formation of a strong pre-reactive complex driving down the barrier height of the insertion step.

We also found another channel that involves a CI insertion in the ROOH, but linking the CI carbon atoms with the inner oxygen atom rather than the outer O-atom. This leads to the formation of an alcohol or ether oxide, as depicted earlier. In good agreement with the B3LYP calculations by Schalley et al.,[52] we find that alcohol oxides, RO(O)H have a low barrier of less than 10 kcal mol^{-1} for H-migration, forming the corresponding ROOH hydroperoxide product. For ether oxides, RO(O)R', we found that the oxide is significantly more stable, and that re-isomerisation to the alkylperoxide ROOR' has a high barrier exceeding 20 kcal mol^{-1}. Schalley et al.[52] have extensive calculations on the isomerisation and dissociation pathways available for alcohol and ether oxides; for the current work we focus only on the lowest energy pathways. For the H_2COO + CH_3OOH reaction, the barrier for formation of the ether oxide is lower than for the insertion channel, by almost 2 kcal mol^{-1}, while for

$(CH_3)_2COO$ the ether oxide channel has a barrier higher by 0.6 kcal mol^{-1}. Redissociation of the ether oxide to the pre-reactive complex is over 10 kcal mol^{-1}, compared to ≤ 5 kcal mol^{-1} for alcohol oxides.

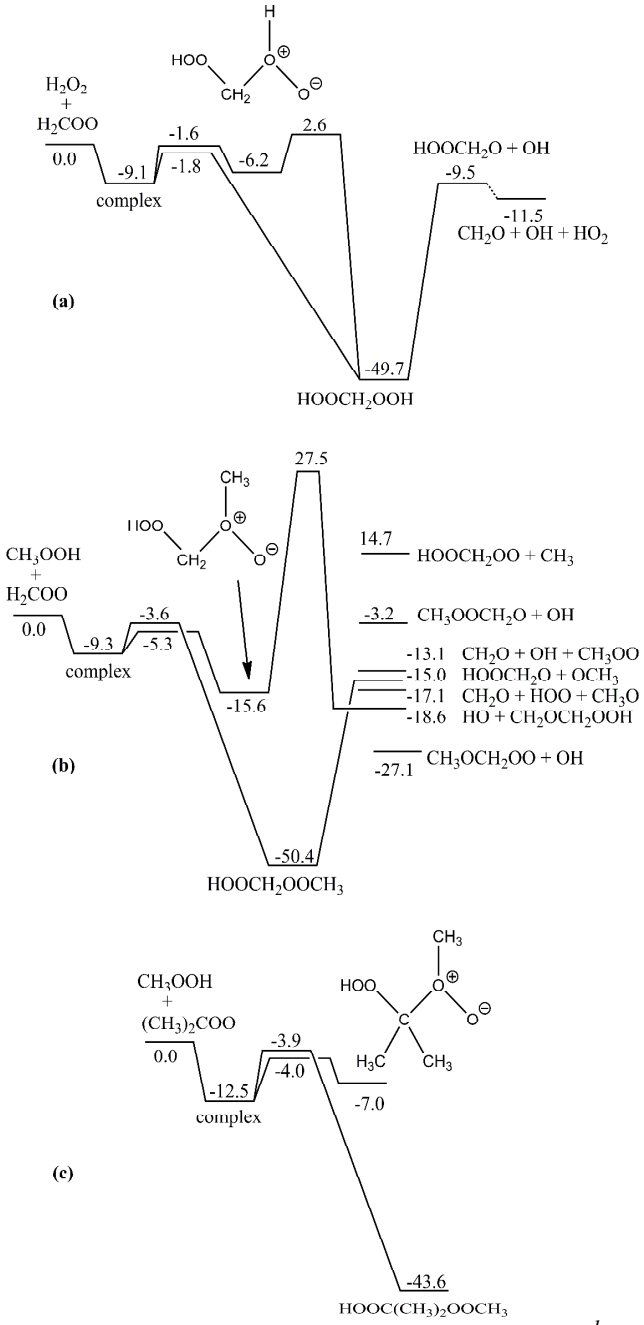

Figure 2: Potential energy surfaces (kcal mol^{-1}) for (a) $CH_2OO + H_2O_2$, (b) $CH_2OO + CH_3OOH$, and (c) $(CH_3)_2COO + CH_3OOH$, at the CCSD(T)/aug-cc-pVTZ//M06-2X/aug-cc-pVTZ level of theory.

4.b. Reaction kinetics

The rate coefficients of the CI + ROOH/HOOH reactions are listed in Table 2. As is typical for a submerged TS in the rate-determining step, the rate coefficients show a negative temperature dependence. The reactions are not very fast, with k(T) ≤ 7×10^{-12} cm^3 $molecule^{-1}$ s^{-1} at 300K and ≤ 4×10^{-11} cm^3 $molecule^{-1}$ s^{-1} at 250 K. With H_2O_2 and ROOH atmospheric concentrations in the ppb range,[40–42,66] the hydroperoxide reaction appears to be a minor loss process for CI. In the experimental conditions from Sakamoto et al.,[43] with significantly higher reactant concentrations than the atmosphere, our results support the proposed CI + ROOH reaction as a source of low-volatility oligomers. The formation of ether oxides was not considered in the experimental work of Sakamoto et al,[43] though our results indicate that alcohol and ether oxides can constitute a significant fraction of the nascent product yield, up to 85% (see Table 2).

Table 2: Rate coefficients k(T) (cm^3 $molecule^{-1}$ s^{-1}) for the reaction of CI with ROOH, where the Arrhenius expression is valid for T=250-350K. The yield of ether oxides listed here is derived from the relative rate across the two entrance TS.

Reaction	k(298 K)	k(T)	Yield ether oxide
CH_2OO + HOOH	3×10^{-13}	1.3×10^{-14} exp(900/T)	28 %
CH_2OO + CH_3OOH	6×10^{-12}	1.1×10^{-15} exp(2590/T)	85 %
$(CH_3)_2COO$ + CH_3OOH	8×10^{-13}	2.4×10^{-15} exp(1740/T)	6 %

4.c Subsequent reactions of ether oxides

Alcohol oxides are found to be comparatively unstable,[52] with an isomerisation channel for H-migration accessible with a barrier below 10 kcal mol^{-1}, and for the hydroperoxide-alcohol oxides discussed in this paper, redissociation to CI + H_2O_2 complex requires less than 5 kcal mol^{-1}. The lifetime of the alcohol oxide intermediates is thus very short, and redissociation to the complex is their most likely fate. Given that formation of the dihydroperoxide adduct is the lowest accessible channel from this complex, and that a 1,2-H-migration leads to the same adduct, we conclude that the reaction of CI with H_2O_2 leads near-exclusively to a dihydroperoxide >C(OOH)OOH.

Ether oxides formed from CI + alkyl hydroperoxides are significantly more stable, and the formation TS is similar or even lower in energy compared to the insertion process. With high-pressure unimolecular decomposition rates of ~10^5 s^{-1} towards the CI + ROOH complex, the ether oxides have a comparatively short lifetime to undergo bimolecular reactions. We are not aware of any literature data concerning ether oxide reaction kinetics, so we performed some preliminary calculations for some potentially interesting reactions.

For the reaction of ether oxides with water, present in high concentrations in the troposphere, we found the formation of a pre-reactive complex with an 8 kcal mol^{-1} stability. However, we were unable to find any kinetically viable transition state beyond this complex formation. The formation of oxywater + carbonyl, or of 2 OH radicals + carbonyl is endothermic by ~20 kcal mol^{-1}, and is energetically not accessible. The formation of a carbonyl compound with HOOH is exothermic by 26 kcal mol^{-1}, but no viable TS could be found for its direct formation. Specifically, the geometric re-arrangements necessary to form HOOH from the oxide are highly complex, and it appears that formation of HOOH would proceed essentially via the formation of 2 OH radicals that recombine, a process that entails a significant energetic barrier. Contrary to carbonyl oxides, ether oxides can not

undergo an insertion reaction into a water O–H bond, such that adduct formation is also not a viable reaction channel. From this, we tentatively conclude that ether oxides are not reactive towards water in the gas phase. The reactivity towards the water dimer was not examined; a concerted migration of several H-atoms could catalyze the reaction, as it does for e.g.[50] the HOOH to H_2OO isomerisation.

As ether oxides are expected to be strong oxidants,[52] we also examined the reaction of $HOOCH_2O(O)CH_3$ with SO_2, to assess its role as a source of SO_3. Ether oxides form a strong pre-reactive complex with SO_2, with a stability of 9 kcal mol^{-1}, and then form SO_3 + a carbonyl compound after clearing a submerged barrier 1.7 kcal mol^{-1} below the free reactants. This mechanism is different to the CI + SO_2 reaction, which proceeds[30] without a barrier directly to a secondary ozonide, which decomposes in a two-step process to yield SO_3. The rate coefficient for $HOOCH_2O(O)CH_3$ + SO_2 is rather low, k(298 K) = 2×10^{-13} cm^3 $molecule^{-1}$ s^{-1}. Extremely high concentrations of SO_2 would thus be necessary to act as a sink for hydroperoxide ether oxides competitive to unimolecular decomposition.

While the current study does not provide full insight into the ether oxide chemistry, it appears that the short lifetime of ether oxides, and the comparatively low concentrations of co-reactants, make it unlikely that ether oxides will undergo bimolecular reactions in the atmosphere. As such, the formation of ether oxides in the CI + ROOH reaction acts mostly as a reservoir for the pre-reactive complex, and the chain adduct will be the dominant if not exclusive product of the CI + ROOH reaction.

5. CI + CO

Table 3: Relative energies (kcal mol^{-1}) for intermediates and transition states in the CH_2OO + CO reaction as depicted in Figure 3. The first header row indicates the level of theory used for geometry optimization, the second for single point energy calculations; scaled M06-2X/aug-cc-pVTZ ZPE-corrections are used throughout. Levels of theory used: M06-2X/aug-cc-pVTZ (M06-2X/aVTZ), CCSD(T)/aug-cc-pVTZ (CC/aVTZ), and CCSD(T) energy extrapolations to infinite basis set used the aug-Schwartz6(DTQ) scheme (CC/aSchw6). Additional energies and geometries can be found in the supporting information.

Structure	M06-2X/aVTZ M06-2X/aVTZ	M06-2X/aVTZ CC/aSchw6	CC/aVTZ CC/aVTZ	CC/aVTZ CC/aSchw6
CH_2OO + CO	0.0	0.0	0.0	0.0
Prereactive complexes	-2.6	-1.7		
TS1	8.7	10.4	10.1	10.1
TS2	11.1	12.5	12.0	12.0
TS3	12.4	13.5		
TS4	35.1			
TS5	35.7			
cyc-$CH_2OOC(=O)$-	-44.2	-40.1		
TS6	-25.2			
CH_2O + CO_2	-122.6	-120.3		

Table 4: Relative energies (kcal mol^{-1}) for intermediates and transition states in the CI + CO reactions at the M06-2X/aug-cc-pVTZ and single point CCSD(T)/aug-cc-pVTZ levels of theory.

Structure	M06-2X/aVTZ	CCSD(T)/aVTZ//M06-2X
syn-CH_3CHOO + CO	0.0	0.0
Prereactive complexes	-2.4	-2.1
TS1	14.8	15.0
TS2	12.6	11.1

TS3	14.8	15.6
TS vinylperformate	31.8	35.5
cyc-$CH(CH_3)OOC(=O)$-	-37.2	-34.9
CH_2=CHOOCHO	-29.0	-23.6
acetaldehyde + CO_2	-119.0	-115.1
anti-CH_3CHOO + CO	0.0	0.0
Prereactive complexes	-2.9	-2.6
TS1	8.9	9.4
TS2	10.6	9.0
TS3	9.7	10.6
cyc-$CH(CH_3)OOC(=O)$-	-40.5	-38.4
acetaldehyde + CO_2	-122.3	-118.6
$(CH_3)_2COO$ + CO	0.0	0.0
Prereactive complexes	-2.7	-2.5
TS1	14.9	14.7
TS2	13.7	14.0
TS3	11.7	9.7
TS vinylperformate	31.4	34.4
cyc-$C(CH_3)_2OOC(=O)$-	-34.2	-33.4
CH_2=$C(CH_3)$OOCHO	-26.5	-21.8
Acetone + CO_2	-117.7	-114.2

Table 5: Barrier heights (kcal mol^{-1}) relative to the separated reactants for unimolecular reactions of SCI, with and without a CO complex in the TS. The levels of theory are M06-2X/aug-cc-pVTZ and single point CCSD(T)/aug-cc-pVTZ on the M06-2X geometries. Scaled M06-2X ZPE energies are used throughout.

Reaction	M06-2X/aVTZ	CCSD(T)/aVTZ//M06-2X
$CH_2OO \rightarrow$ dioxirane	21.4	18.6
CH_2OO + CO $\rightarrow$ dioxirane + CO	19.0	17.0
$CH_2OO \rightarrow$ $^{\bullet}$CHO + $^{\bullet}$OH (1,3 H-shift)	30.4	30.3

$CH_2OO + CO \rightarrow {}^{\bullet}CHO + {}^{\bullet}OH + CO$ (1,3 H-shift)	29.6	29.4
syn-$CH_3CHOO \rightarrow$ dioxirane	25.3	23.2
syn-$CH_3CHOO + CO \rightarrow$ dioxirane + CO	22.7	21.1
syn-$CH_3CHOO \rightarrow$ vinylhydroperoxide	15.3	16.4
syn-$CH_3CHOO + CO \rightarrow$ vinylhydroperoxide + CO	13.6	14.8
anti-$CH_3CHOO \rightarrow$ dioxirane	17.9	15.2
anti-$CH_3CHOO + CO \rightarrow$ dioxirane + CO	15.5	13.2
$(CH_3)_2COO \rightarrow$ dioxirane	22.5	20.4
$(CH_3)_2COO + CO \rightarrow$ dioxirane + CO	20.0	18.2
$(CH_3)_2COO \rightarrow$ vinylhydroperoxide	15.0	15.7
$(CH_3)_2COO + CO \rightarrow$ vinylhydroperoxide + CO	12.0	13.7

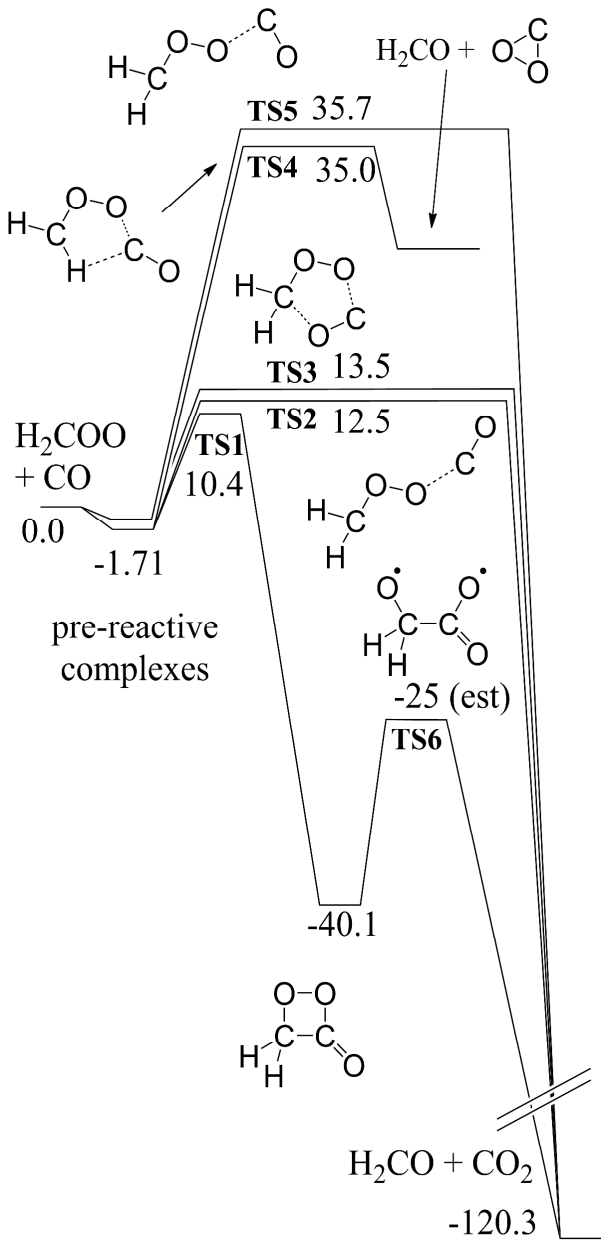

*Figure 3: Potential energy surface (kcal mol^{-1}) for the H_2COO + CO reaction at the CCSD(T)/aug-Schwartz6(DTQ)//M06-2X/aug-cc-pVTZ level of theory. The high-lying **TS4** and **TS5** are shown using M06-2X energies.*

5.a. Potential energy surface

Figure 3 shows the potential energy surface for the reaction of H_2COO with CO, and selected relative energies of the intermediates and TS at various levels of theory are listed in Table 3, with additional results available in the supporting information. Four pre-reactive complexes were found, all within a 1.5 kcal mol^{-1} energy window ; even the most stable complex, at -1.7 kcal mol^{-1} at the CCSD(T)/aug-Schwartz(DTQ) level of theory, is only very weakly bonded, and given the high barriers to reaction, these complexes carry no kinetic significance. In contrast to Kumar et al,[34] who identified only the direct O-transfer from CI to CO, we have identified three routes for the formation of CO_2 + carbonyl, i.e. a cycloaddition pathway over a four-membered ring followed by ring opening (**TS1**), a linear O-transfer TS forming CO_2 directly (**TS2**), and a cycloaddition pathway over a transient five-membered ring structure that dissociates spontaneously to CO_2 + carbonyl (**TS3**). Of these routes, the cycloaddition route **TS1** was found to have the lowest energy barrier for CH_2OO, and the results across the different levels of theory applied are very similar. The difference between the M06-2X and CCSD(T) levels of theory lies mainly in a lower predicted energy of the reactants at the CCSD(T) level, which shifts all relative energies. The energy of the lowest entrance **TS1** based on CCSD(T)/aug-cc-pVTZ single point energy calculations all lie between 9.9 and 10.4 kcal mol^{-1} above the reactants, whereas the aug-Schwartz6(DTQ) energies range from 10.4 to 10.6 kcal mol^{-1}, indicating that our predictions are quite robust against changes in the geometry and basis set (see also supporting information). T1 diagnostics for the lowest three entrance TS are between 0.029 and 0.036, suggesting that the wavefunctions are probably not affected too strongly by multi-reference effects. The geometry and energy of **TS6** for ring-breaking and further dissociation of the four-membered ring cyc-$CH_2OOC(O)$- suffered strongly from spin-contamination and delocalization issues, and can not be described reliably at our chosen level of theory (see also supporting information); as it is not critical to

the current discussion, we opted not to investigate this TS further.

Some additional TS were characterized, proceeding over a transient H_2COOCO structure : **TS4** forms cyclic-CO_2, a high-energy isomer[67–69] of CO_2 with a barrier of 35 kcal mol^{-1} ; this structure readily breaks the ring, resulting in linear CO_2. The second channel, **TS5**, is a complex rearrangement best described as a 1,4-H-shift in the H_2COOCO structure, leading to partial formation of $HC^{\bullet}O$ + $^{\bullet}OCHO$, which during its fragmentation undergoes the reverse H-migration to form H_2CO + CO_2; this complex process has a high M06-2X barrier of 35.7 kcal mol^{-1}. We can not exclude that this channel can also form formic acid anhydride, observed earlier in the experiments by Su et al.,[70] if the carbon and oxygen radical sites recombine instead of allowing a H-migration, but IRC calculations lead to the H_2CO + CO_2 products. The supporting information lists some additional calculations on formic acid anhydride-related reaction channels. Formation of $HC^{\bullet}O$ + $HOC^{\bullet}O$ is exothermic by 36.5 kcal mol^{-1} at the M06-2X level of theory, but no TS was found for this pathway. Scans of the M06-2X PES for this reaction were inconclusive but suggest a barrier of at least 13 kcal mol^{-1}, well above the cycloaddition.

The PES of substituted SCI + CO reaction is similar, with a selection of barrier heights listed in Table 4. One additional pathway is available for SCI with an alkyl group in *syn*-position, leading to the exothermic formation of a vinylperformate through a H-shift:

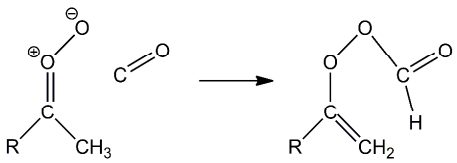

The barrier height for this reaction exceeds 30 kcal mol^{-1}, making this channel unimportant.

5.b. Reaction kinetics

We limit our discussion here to the lowest three reaction pathways, where we find that the lowest

energy path depends on the substitution. As already found for other SCI reactions,[2,63] the higher-energy *anti*-CH_3CHOO conformer shows lower barriers to reaction owing to the release of this potential energy in the transition state.

Table 6: Total rate coefficients k(T) (cm^3 $molecule^{-1}$ s^{-1}) for the CI + CO reaction forming CO_2 either directly or through the cycloadduct, where the Arrhenius expression is valid for T=250-350K.

Reaction	k(298 K)	k(T)
$CH_2OO + CO \rightarrow CH_2O + CO_2$	2×10^{-21}	1.4×10^{-12} exp(-6088/T)
syn-$CH_3CHOO + CO \rightarrow CH_3CHO + CO_2$	7×10^{-21}	5.1×10^{-12} exp(-6069/T)
anti-$CH_3CHOO + CO \rightarrow CH_3CHO + CO_2$	8×10^{-20}	1.3×10^{-12} exp(-4973/T)
$(CH_3)_2COO + CO \rightarrow CH_3C(O)CH_3 + CO_2$	3×10^{-20}	1.4×10^{-12} exp(-5305/T)

The rate coefficients of the CI + CO reactions are listed in Table 6. The reactions are theoretically predicted to be extremely slow, $\leq 1\times10^{-19}$ cm^3 $molecule^{-1}$ s^{-1} at 298K, based on M06-2X/aug-cc-pVTZ rovibrational data, and the highest-quality barrier heights listed in Table 3 and Table 4. This suggests that the direct reaction plays a negligible role in experimental work and especially in the atmosphere. The high level of theory used, and the robustness of the predictions against changes in the level of theory suggests that this result should be reliable.

5.c. Catalysis of SCI unimolecular reactions

In addition to direct reactions, CO could influence the fate of SCI in a reaction mixture by catalyzing unimolecular rearrangements, where ring closure to a dioxirane, and 1,3-H-migration to form a vinylhydroperoxide are the two most common SCI unimolecular rearrangements. Table 5 lists barrier heights for selected SCI unimolecular reactions, both with and without CO present. The change in barrier height upon adding CO is similar to the stability of the pre-reactive complexes of SCI and CO (see Table 3 and Table 4), i.e. the rate of unimolecular re-arrangements within the SCI--CO complex is similar to the rate of uncomplexed SCI, within the accuracy of our calculations. Combined with the weak bonding in the pre-reactive complex, and the concomitantly low equilibrium constant for complexation, this indicates that unimolecular decay of SCI--CO complexes will not impact the chemistry. Any significant contribution of catalysis would then result from the bimolecular process, where a collision between an SCI and a CO allows for a rearrangement in the SCI moiety due to the lowering of the effective barrier by the CO spectator. The impact can be estimated from the ratio of the pseudo-first order rate coefficient for CO-assisted rearrangement over uncomplexed unimolecular rearrangement, $k_{CO}(T)[CO] / k_{uni}(T)$, where we use an average energy barrier difference of 2 kcal mol^{-1} between CO-assisted and unimolecular rearrangement as deduced from Table 5. Even for high values of [CO], up to and above 1 atm., this ratio remains well below 10^{-5}, i.e. the 2 kcal mol^{-1} reduction in effective barrier height afforded by the complexation is unable to overcome the entropic disadvantage of the bimolecular process compared to a direct unimolecular rearrangement. Hence, we conclude that CO is unable to catalyze SCI unimolecular reactions to a significant extent at any relevant concentration.

5.d. Experimental evidence for SCI + CO

Understanding of the chemical fate of CH_2OO and other CIs has been advanced with the recent development of direct techniques for SCI detection. However, substantial insight into CI behaviour, in particular relative rates of bimolecular reactions, has also accrued through indirect methods, such as simulation chamber and laboratory relative rate kinetics studies. In this context, CO has been used as both a CI and an OH scavenger in various experimental studies, although CO is not a particularly favoured OH scavenger given its relatively slow reaction with OH (compared with, for example, cyclohexane and 1,3,5-trimethylbenzene) and hence the high concentrations required to ensure near-total OH removal. The impact (or lack thereof) of the presence of CO upon observed product yields in alkene ozonolysis systems therefore provides some constraint upon the possible rate of the CO + CI reaction, as discussed below and summarized in Table 7.

Su et al.[70] used FTIR spectroscopy to study the kinetics and products of the ethene-ozone reaction with various additional reaction partners, including CO. From this they derived a relative rate $k(CH_2OO+CO)/k(CH_2OO+SO_2)$ of 1.8×10^{-3} and an absolute rate of 1.3×10^{-16}. The experiments were conducted at 700 Torr between 291 and 299 K. Reactants used were in the ppm range with [CO] ~ 1.5 %.

Gutbrod *et al.*[71] used very high CO mole fractions (up to 40 %, in a 1 bar total pressure He / O_2 mixture) as a scavenger for OH radicals in the ozonolysis of a range of small alkenes in a small (70 litre) darkened glass reactor, detecting the resulting increase in CO_2 upon addition of CO as a marker for OH formation. The resulting inferred OH yields were similar to some other studies, when defined in terms of O_3 consumed, for some alkenes – pointing to a relatively low upper limit of $k(CO + CI) < 10^{-18}$ cm^3 $molecule^{-1}$ s^{-1} (for equal competition with a CI unimolecular decomposition rate[21,72] of ~10 s^{-1}) – and/or that the products of the CO + CI reaction also lead to the formation of CO_2. However, the observed relative stoichiometry of the alkene and ozone removal was far from that now expected based

on current understanding, and subsequent studies by Horie and Moortgat[73] identified that additional heterogeneous wall reactions forming CO_2 were likely to have occurred, indicating that these data were potentially biased.

Mihelcic *et al*.[74] reported MIESR observation of HO_2 and $HOCH_2CH_2O_2$ radicals in an ethene-ozone flow-tube system. Total HO_x yields obtained from direct HO_2 observations, and OH inferred from $HOCH_2CH_2O_2$ (formed through OH + C_2H_4, in the absence of CO) were in agreement (within 12%) with those obtained from HO_2 observations in the presence of excess CO (at a mixing ratio of 5 %). Following the reasoning above, under the experimental conditions, *i.e.* 295 K and 1 bar total pressure, this observation implies an upper limit of $k(CH_2OO + CO) < 2.5 \times 10^{-19}$ cm^3 molecule^{-1} s^{-1}, for CO in competition with CH_2OO decomposition at an assumed rate of 3 s^{-1},[14,75,76] and assuming the CO + CH_2OO reaction does not lead to HO_x formation – although the reagent levels used were again rather high (*ca*. 5 % CO mixing ratio).

Brauers *et al*.[77] report observations of HCHO formation from ethene ozonolysis in the SAPHIR chamber, and found that HCHO yields were substantially lower than predicted by the MCM (version 3.1) model, in the presence of excess (500 ppm) CO, suggesting that this indicated that the CH_2OO + CO reaction may be *ca*. 250 times slower than the value included in the MCM model (*i.e.* a value of 4.8×10^{-18}, rather than 1.2×10^{-15} cm^3 molecule^{-1} s^{-1}), considering reaction with H_2O as the alternative fate for the SCI. However, the MCM version 3.1 does not include unimolecular SCI decomposition[20,78] or (more importantly) the relatively fast reaction of CH_2OO with the water vapour dimer,[7,13] so the fate of SCI may not be reliably simulated.

Wegener et al.[79] reported radical yields from a range of alkene-ozonolysis reactions, studied in the SAPHIR chamber in the presence and absence of excess (500 ppm) CO, as a function of humidity. Radical yields were inferred indirectly through the excess turnover of the alkene (due to reaction with

OH) and of ozone (due to reaction with HO_2). In the presence of CO, reduced alkene and ozone turnover was observed – attributed to scavenging of OH, but also potentially arising from CO intercepting / reacting with some fraction of the CI population. In contrast to previous and subsequent studies however, an OH yield of 0 (± 0.05) was obtained for ethene, precluding analysis of the type outlined above. Wegener et al. also found an increase in HO_x yields with increasing humidity – in contrast to the results of other work, and a qualitative understanding of radical formation from CI decomposition occurring in competition with bimolecular reactions, such as CI + H_2O. Taken in isolation, this result would suggest that H_2O can effectively compete with CO for SCI – equal reaction of CH_2OO with the water vapour dimer, $(H_2O)_2$, and with CO would imply an upper limit of $k(CH_2OO + CO) < 7.9 \pm 10^{-14}$ cm^3 molecule^{-1} s^{-1} (using the value of $CH_2OO + (H_2O)_2$ from Chao et al.[13]).

Subsequently, Alam *et al*.[47] reported a study of ethene ozonolysis performed in the EUPHORE simulation chamber at rather lower reactant abundance – 500 ppb of ethene and ozone, and with some experiments performed in the presence of excess CO (ca. 500 ppm) as an OH, and SCI, scavenger. In the presence of excess CO, a formaldehyde yield of 1.54 was observed, interpreted to indicate that 54 % of the CI formed (alongside unit HCHO primary carbonyl yield) reacted with CO to form HCHO under the experimental conditions (298 ± 10 K and 1000 ± 50 mbar of scrubbed air). Assuming a single stabilised Criegee intermediate (SCI) with a decomposition rate of 3 s^{-1} this would indicate a lower limit for $k(CH_2OO + CO) = 2.1 \times 10^{-15}$ (value for 90% of the CH_2OO formed to react with CO rather than undergo unimolecular decomposition, assuming that CH_2OO decomposition does not lead to HCHO). Alam *et al*. also observed a reduction in the HO_2 radical yield in the presence of CO, and noted that one explanation for the observed behaviour was bimolecular reactions (in this case, of CO) with a stabilised SCI, in competition with decomposition –the observed reduction in HO_2 yield (from 0.27 to 0.10, as CO increased from <100 ppb to 500 ppm) would correspond to a value for $k(CH_2OO +$

CO) of 4×10^{-16} cm^3 molecule^{-1} s^{-1} (again, assuming competition with a unimolecular decomposition rate of 3 s^{-1}). Finally, Alam *et al*. also observed a reduction in HO_2 yield with an increase in RH from 0.2 % to 29 % in the presence of excess CO – attributed to reaction of H_2O with the SCI, assuming that this reaction does not lead to OH or HO_2 formation. The reduction in HO_x yield with increasing RH implies that H_2O competes effectively with both decomposition and reaction with CO for the SCI – implying an upper limit to $k(CH_2OO + CO)$ of 3.2×10^{-14} cm^3 molecule^{-1} s^{-1}, assuming reaction of SCI with water is dominated by the water dimer, $(H_2O)_2$, with a rate constant of 6.5×10^{-12} cm^3 molecule^{-1} s^{-1}.[13] Similar reductions in HO_2 yield with RH, in excess CO experiments, were also observed[80] for other alkenes, e.g. 2,3-dimethyl-but-2-ene; as SCI + $(H_2O)_2$ reactions are thought to be substantially slower for larger SCIs such as $(CH_3)_2COO$, by 1 - 3 orders of magnitude compared with CH_2OO,[2,63] this observation indicates that the upper limit for k(CO + $(CH_3)_2COO$) must be correspondingly lower.

Table 7: Summary of theoretical work, and experimental work from which CI +CO rate coefficients (cm^3 molecule^{-1} s^{-1}) can be derived.

Reference	*k*(CI+CO)	Conditions	Methodology
This work	2×10^{-21} to 8×10^{-20}	298 K High pressure	Theoretical study on 4 SCI CCSD(T)/aVTZ//M06-2X/aVTZ and CCSD(T)/aug-Schwartz6(DTQ)//CCSD(T)/aVTZ
Kumar et al.[34] (2014)	7×10^{-26} to 2×10^{-20}	298 K High pressure	Theoretical study on 14 SCI CCSD(T)/aVTZ//M06-2X/aVTZ
Su et al.[70] (1980)	1.3×10^{-16} [a]	291 – 299 K 700 Torr [CO] ~ 1.5 %	Ethene + ozone FTIR detailed product study
Gutbrod et al.[71] (1997)	$< 10^{-18}$	1 bar He/O_2 [CO] ≤ 40 %	Alkene + ozone Measured change in [CO_2] as marker for OH formation from CI + CO
Mihelcic et al.[74] (1999)	$< 2.5\times10^{-19}$	295 K 1 bar [CO] ~ 5 %	Ethene + ozone Measured change in HO_x yield (from MIESR observations of HO_2 and $HOCH_2CH_2O_2$)
Brauers et al.[77] (2007)	4.8×10^{-18}	[CO] = 500 ppm	Ethene + ozone Measured change in HCHO yield

Wegener et al.[79] (2007)	$< 7.9\times10^{-14}$	[CO] = 500 ppm	Alkene + ozone Measured change in alkene and ozone turnover rates
Alam et al.[47] (2011)	$> 2.1\times10^{-15}$ [b]	298 K 1000 mbar [CO] = 500 ppm	Ethene + ozone (500 ppb) Measured change in HCHO yield
Alam et al.[47] (2011)	4×10^{-16} [b]	298 K 1000 mbar [CO] = 0.1 – 500 ppm	Ethene + ozone (500 ppb) Measured change in HO_2 yield
Alam et al.[47] (2011)	$< 3.2\times10^{-14}$	298 K 1000 mbar [CO] = excess	Ethene + ozone (500 ppb) Measured change in HO_2 yield as a function of $[H_2O]$

[a] assuming CI unimolecular decomposition rate = 10 s^{-1} [21,72]

[b] assuming CH_2OO unimolecular decomposition rate = 3 s^{-1} [14,75,76]

In summary, the earlier laboratory experiments provide some evidence for a slow rate constant for reaction of CO with SCIs, with upper limits of the order of $10^{-18} – 10^{-19}$ cm^3 $molecule^{-1}$ s^{-1}; however the precursor concentrations used were extremely high, and later work has suggested that heterogeneous and other reactions may have perturbed the results. Subsequent studies, at lower reagent abundance, in large simulation chambers determine upper limits to $k(CH_2OO + CO)$ of the order of $(3 – 7) \times 10^{-14}$ cm^3 $molecule^{-1}$ s^{-1}, and indicate actual values of the order of $10^{-15} – 10^{-16}$ cm^3 $molecule^{-1}$ s^{-1}, although these calculations are directly dependent upon the value assumed for the CH_2OO unimolecular decomposition rate (here, 3 s^{-1}),[14,75,76] and the reactivity of CH_2OO with water vapour (here, assumed to be solely due to $(H_2O)_2$, using the rate obtained by Chao et al.[13]).

6. Conclusions

In this work, we studied the reaction of Criegee intermediates with ozone, hydroperoxides, and CO. The reaction with ozone depends strongly on the substitution and isomer of the CI, with anti-CH_3CHOO yielding the fastest reaction of the CI investigated, 3×10^{-12} cm^3 $molecule^{-1}$ s^{-1}. Using the predicted rate coefficients, it is clear that the CI+O_3 reaction in the troposphere will have a negligible contribution to SCI loss, and is unable to compete effectively against the reactions of CI with H_2O, $(H_2O)_2$, and carboxylic acids, depending on the CI examined.[30,5,21] In laboratory and chamber studies proceeding with higher concentrations of ozone, however, the reaction can have an influence on the concentration of stabilized CI, as shown in a recent modeling study by Novelli et al.,[21] complementing their experimental work, using the CI + O_3 rate coefficients detailed in this work.

The reactions of CI + hydroperoxides, ROOH, and hydrogen peroxide, H_2O_2, were found to possess similar rate coefficients as the reaction with O_3. In general, the concentrations of ROOH and H_2O_2 are lower than those of O_3, and the reaction is not expected to be of critical importance except for some experimental reaction conditions. The predictions in this work support the recent experimental observations by Sakamoto et al.,[43] showing that the CI + ROOH reaction can indeed form oligomers at an appreciable rate, and that this reaction could therefore contribute in the formation of biogenic SOA in low-NOx environments. This reaction complements the CI + RO_2 reaction identified earlier as a source of oligomers.[44,45,30] The CI + ROOH reaction furthermore allows the formation of exotic ether oxides. However, the hydroperoxy-substituted ether oxides formed here were found to be short-lived, and are expected to redissociate to the pre-reactive complex prior to undergoing secondary reactions. The chemistry of ether oxides shows moderately fast reaction with SO_2, while no accessible pathways were found for the reaction with water.

The reaction of CI with carbon monoxide was theoretically predicted to be very slow. While (indirect) experimental work on the CI + CO reaction likewise finds that the reaction is slow, the

values derived by assuming a unimolecular decay rate of 3 s^{-1} and a SCI + $(H_2O)_2$ reaction rate coefficient of 6.5×10^{-12} cm^3 $molecule^{-1}$ s^{-1} remain 4 to 5 orders of magnitude faster than the theoretical values. For the levels of theory used, one does not *a priori* expect an uncertainty on the barrier height of ~6 kcal mol^{-1}, which is what would be needed to bring both sets of data in agreement. Aside from a fundamental breakdown of the quantum chemical methodology, the theoretical work could also be affected by a missing channel with a significantly lower energy barrier. Our extensive searches for such an elusive TS found several exotic, high-energy pathways and characterized a significantly larger part of the PES than the work of Kumar et al.,[34] but even systematic stepwise scans of the PES did not reveal a potential ingress with energies lower than those of **TS1**. The interpretation of the experimental data, in turn, remains uncertain, and depends directly on the rate coefficients assumed for the competing reactions which for the moment still carry a significant uncertainty,[2,14,15,17,20,21,63,72,75,76,78,81] though not necessarily as large as 4 to 5 orders of magnitude. At this time, then, we can not easily reconcile theoretical and experimental data, though both agree that the SCI + CO reaction is of no importance in the troposphere.

Acknowledgments

LV is supported by the Max Planck Graduate Center with the Johannes Gutenberg-Universität Mainz (MPGC). WJB and ARR acknowledge support from the EU FP7 EUROCHAMP 2 Transnational Access activity (E2-2012-05-28-0077), and the UK NERC (NE/K005448/1 and NCAS funding).

References

1. D. Johnson and G. Marston, *Chem. Soc. Rev.*, 2008, **37**, 699–716.
2. L. Vereecken and J. S. Francisco, *Chem. Soc. Rev.*, 2012, **41**, 6259–6293.
3. B. J. Finlayson-Pitts and J. N. Pitts, *Chemistry of the Upper and Lower Atmosphere: Theory, Experiments, and Applications*, Academic Press, San Diego, 1999.
4. C. A. Taatjes, D. E. Shallcross, and C. Percival, *Phys. Chem. Chem. Phys.*, 2014, **16**, 1704–1718.
5. L. Vereecken, H. Harder, and A. Novelli, *Phys. Chem. Chem. Phys.*, 2014, **16**, 4039–4049.
6. Z. J. Buras, R. M. I. Elsamra, A. Jalan, J. E. Middaugh, and W. H. Green, *J. Phys. Chem. A*, 2014, **118**, 1997–2006.
7. A. B. Ryzhkov and P. A. Ariya, *Chem. Phys. Lett.*, 2003, **367**, 423–429.
8. A. B. Ryzhkov and P. A. Ariya, *Phys. Chem. Chem. Phys.*, 2004, **6**, 5042–5050.
9. J. M. Anglada, J. González, and M. Torrent-Sucarrat, *Phys. Chem. Chem. Phys.*, 2011, **13**, 13034–13045.
10. T. Berndt, T. Jokinen, M. Sipilä, R. L. Mauldin, H. Herrmann, F. Stratmann, H. Junninen, and M. Kulmala, *Atmos. Environ.*, 2014, **89**, 603–612.
11. C. A. Taatjes, G. Meloni, T. M. Selby, A. J. Trevitt, D. L. Osborn, C. J. Percival, and D. E. Shallcross, *J. Am. Chem. Soc.*, 2008, **130**, 11883–11885.
12. J. Ahrens, P. T. M. Carlsson, N. Hertl, M. Olzmann, M. Pfeifle, J. L. Wolf, and T. Zeuch, *Angew. Chem. Int. Ed.*, 2014, **53**, 715–719.
13. W. Chao, J.-T. Hsieh, C.-H. Chang, and J. J.-M. Lin, *Science*, 2015, **347**, 751–754.
14. T. Berndt, T. Jokinen, R. L. Mauldin, T. Petäjä, H. Herrmann, H. Junninen, P. Paasonen, D. R. Worsnop, and M. Sipilä, *J. Phys. Chem. Lett.*, 2012, **3**, 2892–2896.
15. T. Berndt, J. Voigtländer, F. Stratmann, H. Junninen, R. L. Mauldin III, M. Sipilä, M. Kulmala, and H. Herrmann, *Phys. Chem. Chem. Phys.*, 2014, **16**, 19130–19136.
16. Z. J. Buras, R. M. I. Elsamra, and W. H. Green, *J. Phys. Chem. Lett.*, 2014, **5**, 2224–2228.
17. R. Chhantyal-Pun, A. Davey, D. E. Shallcross, C. J. Percival, and A. J. Orr-Ewing, *Phys. Chem. Chem. Phys.*, 2014, **17**, 3617–3626.
18. T. R. Lewis, M. A. Blitz, D. E. Heard, and P. W. Seakins, *Phys. Chem. Chem. Phys.*, 2015, **17**, 4859–4863.
19. F. Liu, J. M. Beames, A. S. Petit, A. B. McCoy, and M. I. Lester, *Science*, 2014, **345**, 1596–1598.
20. M. J. Newland, A. R. Rickard, M. S. Alam, L. Vereecken, A. Muñoz, M. Ródenas, and W. J. Bloss, *Phys. Chem. Chem. Phys.*, 2015, **17**, 4076–4088.
21. A. Novelli, L. Vereecken, J. Lelieveld, and H. Harder, *Phys. Chem. Chem. Phys.*, 2014, **16**, 19941–19951.
22. B. Ouyang, M. W. McLeod, R. L. Jones, and W. J. Bloss, *Phys. Chem. Chem. Phys.*, 2013, **15**, 17070–17075.
23. L. Sheps, A. M. Scully, and K. Au, *Phys. Chem. Chem. Phys.*, 2014, **16**, 26701–26706.
24. D. Stone, M. Blitz, L. Daubney, N. U. M. Howes, and P. Seakins, *Phys. Chem. Chem. Phys.*, 2014, **16**, 1139–1149.
25. C. A. Taatjes, O. Welz, A. J. Eskola, J. D. Savee, D. L. Osborn, E. P. F. Lee, J. M. Dyke, D. W. K. Mok, D. E. Shallcross, and C. J. Percival, *Phys. Chem. Chem. Phys.*, 2012, **14**, 10391–10400.
26. C. A. Taatjes, O. Welz, A. J. Eskola, J. D. Savee, A. M. Scheer, D. E. Shallcross, B. Rotavera, E. P. F. Lee, J. M. Dyke, D. K. W. Mok, D. L. Osborn, and C. J. Percival, *Science*, 2013, **340**, 177–180.
27. W.-L. Ting, C.-H. Chang, Y.-F. Lee, H. Matsui, Y.-P. Lee, and J. J.-M. Lin, *J. Chem. Phys.*, 2014, **141**, 104308.
28. O. Welz, J. D. Savee, D. L. Osborn, S. S. Vasu, C. J. Percival, D. E. Shallcross, and C. A. Taatjes, *Science*, 2012, **335**, 204–207.
29. O. Welz, A. J. Eskola, L. Sheps, B. Rotavera, J. D. Savee, A. M. Scheer, D. L. Osborn, D. Lowe, A.

Murray Booth, P. Xiao, M. Anwar H. Khan, C. J. Percival, D. E. Shallcross, and C. A. Taatjes, *Angew. Chem.*, 2014, **126**, 4635–4638.
30. L. Vereecken, H. Harder, and A. Novelli, *Phys. Chem. Chem. Phys.*, 2012, **14**, 14682–14695.
31. J. M. Anglada, S. Olivella, and A. Solé, *Phys. Chem. Chem. Phys.*, 2013, **15**, 18921–18933.
32. A. Jalan, J. W. Allen, and W. H. Green, *Phys. Chem. Chem. Phys.*, 2013, **15**, 16841–16852.
33. H. G. Kjaergaard, T. Kurtén, L. B. Nielsen, S. Jørgensen, and P. O. Wennberg, *J. Phys. Chem. Lett.*, 2013, 2525–2529.
34. M. Kumar, D. H. Busch, B. Subramaniam, and W. H. Thompson, *J. Phys. Chem. A*, 2014, **118**, 1887–1894.
35. W. Wei, R. Zheng, Y. Pan, Y. Wu, F. Yang, and S. Hong, *J. Phys. Chem. A*, 2014, **118**, 1644–1650.
36. S. Jørgensen and A. Gross, *J. Phys. Chem. A*, 2009, **113**, 10284–10290.
37. P. Aplincourt and M. F. Ruiz-López, *J. Am. Chem. Soc.*, 2000, **122**, 8990–8997.
38. A. Mansergas, J. González, M. Ruiz-López, and J. M. Anglada, *Comput. Theor. Chem.*, 2011, **965**, 313–320.
39. B. Long, X. Tan, Z. Long, Y. Wang, D. Ren, and W. Zhang, *J. Phys. Chem. A*, 2011, **115**, 6559–6567.
40. M. H. Lee, B. G. Heikes, and D. W. O'Sullivan, *Atmos. Environ.*, 2000, **34**, 3475–3494.
41. L. J. Nunnermacker, J. B. Weinstein-Lloyd, B. Hillery, B. Giebel, L. I. Kleinman, S. R. Springston, P. H. Daum, J. Gaffney, N. Marley, and G. Huey, *Atmospheric Chem. Phys.*, 2008, **8**, 7619–7636.
42. T. Klippel, H. Fischer, H. Bozem, M. G. Lawrence, T. Butler, P. Joeckel, H. Tost, M. Martinez, H. Harder, E. Regelin, R. Sander, C. L. Schiller, A. Stickler, and J. Lelieveld, *Atmospheric Chem. Phys.*, 2011, **11**, 4391–4410.
43. Y. Sakamoto, S. Inomata, and J. Hirokawa, *J. Phys. Chem. A*, 2013, **117**, 12912–12921.
44. A. Sadezky, P. Chaimbault, A. Mellouki, A. Römpp, R. Winterhalter, G. Le Bras, and G. K. Moortgat, *Atmospheric Chem. Phys.*, 2006, **6**, 5009–5024.
45. A. Sadezky, R. Winterhalter, B. Kanawati, A. Römpp, B. Spengler, A. Mellouki, G. Le Bras, P. Chaimbault, and G. K. Moortgat, *Atmospheric Chem. Phys.*, 2008, **8**, 2667–2699.
46. L. Vereecken, H. Harder, and A. Novelli, in *European Geosciences Union Generaly Assembly*, Vienna, Austria, 2013.
47. M. S. Alam, M. Camredon, A. R. Rickard, T. Carr, K. P. Wyche, K. E. Hornsby, P. S. Monks, and W. J. Bloss, *Phys. Chem. Chem. Phys.*, 2011, **13**, 11002.
48. D. Schröder, C. A. Schalley, N. Goldberg, J. Hrûsák, and H. Schwarz, *Chem.- Eur. J.*, 1996, **2**, 1235–1242.
49. Y. Ge, K. Olsen, R. I. Kaiser, and J. D. Head, in *AIP Conference Proceedings*, Honolulu, Hawaii (USA), 2006, pp. 253–259.
50. T. Okajima, *Can. J. Chem.*, 2001, **79**, 22–28.
51. T. Okajima, *J. Mol. Struct.-Theochem*, 2001, **572**, 45–52.
52. C. A. Schalley, J. N. Harvey, D. Schröder, and H. Schwarz, *J. Phys. Chem. A*, 1998, **102**, 1021–1035.
53. Y. Zhao and D. G. Truhlar, *Theor. Chem. Acc.*, 2008, **120**, 215–241.
54. T. H. Dunning, *J. Chem. Phys.*, 1989, **90**, 1007–1023.
55. G. D. Purvis and R. J. Bartlett, *J. Chem. Phys.*, 1982, **76**, 1910.
56. M. Rittby and R. J. Bartlett, *J. Phys. Chem.*, 1988, **92**, 3033–3036.
57. J. M. L. Martin, *Chem. Phys. Lett.*, 1996, **259**, 669–678.
58. I. M. Alecu, J. Zheng, Y. Zhao, and D. G. Truhlar, *J. Chem. Theory Comput.*, 2010, **6**, 2872–2887.
59. J. Zheng, I. M. Alecu, B. J. Lynch, Y. Zhao, and D. G. Truhlar, .
60. L. Noodleman, *J. Chem. Phys.*, 1981, **74**, 5737–5743.
61. L. Noodleman and E. R. Davidson, *Chem. Phys.*, 1986, **109**, 131–143.
62. D. K. Malick, G. A. Petersson, and J. A. Montgomery, *J. Chem. Phys.*, 1998, **108**, 5704–5713.

63. L. Vereecken, D. R. Glowacki, and M. J. Pilling, *Chem. Rev.*, 2015, **115**, 4063–4114.
64. J. C. Rienstra-Kiracofe, W. D. Allen, and H. F. Schaefer, *J. Phys. Chem. A*, 2000, **104**, 9823–9840.
65. M. J. Frisch, G. W. Trucks, H. B. Schlegel, G. E. Scuseria, M. A. Robb, J. R. Cheeseman, G. Scalmani, V. Barone, B. Mennucci, G. A. Petersson, H. Nakatsuji, M. Caricato, X. Li, H. P. Hratchian, A. F. Izmaylov, J. Bloino, G. Zheng, J. L. Sonnenberg, M. Hada, M. Ehara, K. Toyota, R. Fukuda, J. Hasegawa, M. Ishida, T. Nakajima, Y. Honda, O. Kitao, H. Nakai, T. Vreven, J. A. Montgomery Jr., J. E. Peralta, F. Ogliaro, M. Bearpark, J. J. Heyd, E. Brothers, K. N. Kudin, V. N. Staroverov, T. Keith, R. Kobayashi, J. Normand, J. Normand, K. Raghavachari, A. Rendell, J. C. Burant, S. S. Iyengar, J. Tomasi, M. Cossi, N. Rega, J. M. Millam, M. Klene, J. E. Knox, J. B. Cross, V. Bakken, C. Adamo, J. Jaramillo, R. Gomperts, R. E. Stratmann, O. Yazyev, A. J. Austin, R. Cammi, C. Pomelli, J. W. Ochterski, R. L. Martin, K. Morokuma, V. G. Zakrzewski, G. A. Voth, P. Salvador, J. J. Dannenberg, S. Dapprich, A. D. Daniels, O. Farkas, J. B. Foresman, J. V. Ortiz, J. Cioslowski, D. J. Fox, and J. A. Pople, *Gaussian 09, Revision B.01*, Gaussian Inc., Wallington CT, 2010.
66. K. Hens, A. Novelli, M. Martinez, J. Auld, R. Axinte, B. Bohn, H. Fischer, P. Keronen, D. Kubistin, A. C. Nölscher, R. Oswald, P. Paasonen, T. Petäjä, E. Regelin, R. Sander, V. Sinha, M. Sipilä, D. Taraborrelli, C. Tatum Ernest, J. Williams, J. Lelieveld, and H. Harder, *Atmospheric Chem. Phys.*, 2014, **14**, 8723–8747.
67. D. Feller, J. Katriel, and E. R. Davidson, *J. Chem. Phys.*, 1980, **73**, 4517–4520.
68. S. S. Xantheas and K. Ruedenberg, *Int. J. Quantum Chem.*, 1994, **49**, 409–427.
69. S. Y. Grebenshchikov, *J. Chem. Phys.*, 2013, **138**, 224107.
70. F. Su, J. G. Calvert, and J. H. Shaw, *J. Phys. Chem.*, 1980, **84**, 239–246.
71. R. Gutbrod, S. Meyer, M. M. Rahman, and R. N. Schindler, *Int. J. Chem. Kinet.*, 1997, **29**, 717–723.
72. J. D. Fenske, A. S. Hasson, A. W. Ho, and S. E. Paulson, *J. Phys. Chem. A*, 2000, **104**, 9921–9932.
73. O. Horie and G. K. Moortgat, *Chem. Phys. Lett.*, 1998, **288**, 464–472.
74. D. Mihelcic, M. Heitlinger, D. Kley, P. Musgen, and A. Volz-Thomas, *Chem. Phys. Lett.*, 1999, **301**, 559–564.
75. O. Horie, P. Neeb, and G. K. Moortgat, *Int. J. Chem. Kinet.*, 1997, **29**, 461–468.
76. O. Horie, C. Schafer, and G. K. Moortgat, *Int. J. Chem. Kinet.*, 1999, **31**, 261–269.
77. T. Brauers, J. Bossmeyer, H.-P. Dorn, E. Schlosser, R. Tillmann, R. Wegener, and A. Wahner, *Atmospheric Chem. Phys.*, 2007, **7**, 3579–3586.
78. M. Olzmann, E. Kraka, D. Cremer, R. Gutbrod, and S. Andersson, *J. Phys. Chem. A*, 1997, **101**, 9421–9429.
79. R. Wegener, T. Brauers, R. Koppmann, S. Rodriguez Bares, F. Rohrer, R. Tillmann, A. Wahner, A. Hansel, and A. Wisthaler, *J. Geophys. Res.-Atmospheres*, 2007, **112**, D13301.
80. M. S. Alam, A. R. Rickard, M. Camredon, K. P. Wyche, T. Carr, K. E. Hornsby, P. S. Monks, and W. J. Bloss, *J. Phys. Chem. A*, 2013, **117**, 12468–12483.
81. K. T. Kuwata, M. R. Hermes, M. J. Carlson, and C. K. Zogg, *J. Phys. Chem. A*, 2010, **114**, 9192–9204.